Supporting Information for

Observation of Electron Shakeup in CdSe/CdS Core/Shell Nanoplatelets

Felipe V. Antolinez, Freddy T. Rabouw,[§] Aurelio A. Rossinelli, Jian Cui,[#] and David J. Norris[*]

Optical Materials Engineering Laboratory, Department of Mechanical and Process Engineering,
ETH Zurich, 8092 Zurich, Switzerland

[*]E-mail: dnorris@ethz.ch

S1. Sample Fabrication

Fabrication of samples for low-temperature spectroscopy. The synthesis of the core/shell CdSe/CdS NPLs was performed as described by Rossinelli et al.[1] In these NPLs, square CdSe cores of ~20 nm side length and a thickness of four monolayers (~1.2 nm) are uniformly surrounded by a shell of ~12 ML (~3.5 nm) CdS. For single-particle measurements, 70 µL of a dilute dispersion of NPLs in hexane was spin-coated at 2500 r.p.m onto intrinsic crystalline Si wafers with a 3-µm-thick thermal-oxide layer to obtain a surface coverage of $< 0.1\ \mu m^{-2}$. For the ensemble measurement in Figure 1a, a small drop of concentrated stock dispersion was drop-casted onto the Si substrate.

S2. Optical Measurements

Experimental setup. The experimental setup, which allows multiple excitation and detection schemes, is shown in Figure S1. The sample is mounted on a piezo positioning system (Attocube, 1×ANPz101 and 2×ANPx101) inside a closed-cycle helium cryostat (Montana Instruments, Cryostation 2 with LWD option). To excite NPLs, a 405-nm laser diode (Picoquant, D-C-405) was operated at a repetition rate of 40 MHz and directed to the sample using a dichroic beam splitter (405-nm long pass, Omega Filters).

The emission from the sample was collected with a 60× extra-long-working-distance (ELWD) objective [Nikon, CFI S P-Fluor ELWD with a numerical aperture (NA) of 0.7] and sent through the beam splitter and relay lenses (focal length of 200 mm) into an imaging spectrometer (Andor, Shamrock 303i). The emission was dispersed with a grating of 300 lines/mm (500-nm blaze) and imaged with an air-cooled electron-multiplying charged-coupled device (EMCCD) camera (Andor, iXon 888 Ultra). For fluorescence measurements, an emission filter (450-nm long pass, AHF analysentechnik) was placed directly after the dichroic beam splitter to filter out the 405-nm excitation light. For time-resolved measurements, a 50/50 broadband beam splitter cube (Thorlabs, BS013) was placed in the path before the spectrograph and half of the emission was focused onto an avalanche photodiode (Excelitas, SPCM-AQRH-14-TR) connected to a time-tagger box (Picoquant, HydraHarp 400) for time-correlated single-photon counting (TCSPC). The camera shutter signal was connected to the marker input of the time-tagger box to correlate photon arrival times with the camera frame number.

S3. Data Analysis

Data preprocessing and spectral sorting. All data processing and analysis was performed in the Python programming language. For the analysis of the spectral frames, a background time series, recorded with identical settings, but with no laser excitation, was subtracted from the raw data, and the few defective EMCCD pixels were removed from each spectrum. Then, the k-means clustering algorithm from the scikit-learn machine-learning library[2] was used to sort the data into a given number of clusters without any further preprocessing.

Peak energy separation histograms. To extract the histogram of peak energy separations, the data was first sorted into a given number of clusters. Then, the peak-finder algorithm from the scipy Python library was used to decide how many emission peaks are present in the average spectrum of each cluster and to determine the starting values for the fits to the individual frames. The spectrum from each individual frame was then fit with the corresponding number of Lorentzian peaks. For the histogram, the energy separations between all resulting peaks were counted and aggregated for all frames.

S4. Modeling

Modeling the single-electron excited states in the potential of a surface charge. The single-electron states in the potential of a single positive charge on the CdS surface were calculated by application of the variational principle in an effective-mass framework.[3] The electron wavefunctions and energies are obtained by solving the following Schrödinger equation:

$$\left(-\frac{\hbar}{2m_{\parallel}^{\mathrm{e}}}\left(\frac{\partial^2}{\partial x^2}+\frac{\partial^2}{\partial y^2}\right)-\frac{\hbar}{2m_{z}^{\mathrm{e}}}\frac{\partial^2}{\partial z^2}+V_{\mathrm{conf}}^{\mathrm{e}}(x,y,z)+V_{\mathrm{ext}}^{\mathrm{e}}(x,y,z)\right)\Psi=E\Psi\ ,$$

where x and y are the in-plane coordinates, z is the out-of-plane coordinate, and $m_{\parallel}^{\mathrm{e}}$ and m_{z}^{e} refer to the in-plane and out-of-plane effective masses,[4] respectively. The electron wave function Ψ

$$\Psi(x,y,z)=\sum_{l,m,n}c_{l,m,n}\psi_{l,m,n}(x,y,z)$$

is expanded as a superposition of orthogonal particle-in-a-box wave functions inside the core NPL:

$$\psi_{l,m,n}(x,y,z)=\sqrt{\frac{8}{L_xL_yL_z}}\sin\left(\frac{l\pi}{L_x}x\right)\ \sin\left(\frac{m\pi}{L_y}y\right)\sin\left(\frac{n\pi}{L_z}(z-d_{\mathrm{shell}})\right),$$

where $c_{l,m,n}$ are the expansion coefficients, and L_x, L_y, and L_z are the core NPL dimensions in x-, y-, and z-direction, respectively, and d_{shell} is the thickness of the shell. Outside of the core material, the wave function is zero.

The particle-in-a-box confinement potential is

$$V_{\mathrm{conf}}^{\mathrm{e}}(x,y,z)=0\ \ \text{for}\ \begin{cases}0\le x\le L_x\\ 0\le y\le L_y\\ d_{\mathrm{shell}}\le z\le d_{\mathrm{shell}}+L_z\end{cases}$$

and $V_{\mathrm{conf}}^{\mathrm{e}}(x,y,z)=\infty$ outside the NPL core domain. The interaction potential between a charge on the shell surface and the electron inside the core is calculated with the method of image charges in the 2D-limit to take into account the dielectric effect:[5]

$$V_{\mathrm{ext}}^{\mathrm{e}}(x,y,z) = -\frac{1}{4\pi\varepsilon_0}\left[\frac{2\varepsilon_1}{\varepsilon_1+\varepsilon_2}\right]\sum_{n=0}^{\infty}\frac{q_n e^2}{\varepsilon_1\sqrt{(x-x_{\mathrm{sc}})^2+(y-y_{\mathrm{sc}})^2+(z-z_n)^2}}$$

where x_{sc}, y_{sc}, and z_{sc} are the positions of the surface charge, e is the elementary charge, ε_0 is the vacuum permittivity, q_n is defined as

$$q_n = \left[\frac{\varepsilon_1-\varepsilon_2}{\varepsilon_1+\varepsilon_2}\right]^{|n|},$$

ε_1 and ε_2 are the permittivities inside and outside of the NPL, respectively, and z_n are the positions of the images of the surface charge:

$$z_n = \left(n + \frac{1+(-1)^n}{2}\right)(L_z + 2d_{\mathrm{shell}}) + (-1)^n z_{\mathrm{sc}}\,.$$

For the calculations in Figures 4e and 4f of the main text we assumed $\varepsilon_{\mathrm{CdSe}} = \varepsilon_{\mathrm{CdS}} = \varepsilon_1$. The values of all parameters are given in Table S1. We expanded the orthogonal basis functions up to orders $l = m = 17$, and $n = 1$ due to the strong confinement in the z-direction.

S5. Supplementary References

(1) Rossinelli, A. A.; Riedinger, A.; Marqués-Gallego, P.; Knüsel, P. N.; Antolinez, F. V.; Norris, D. J. High-Temperature Growth of Thick-Shell CdSe/CdS Core/Shell Nanoplatelets. *Chem. Commun.* **2017**, *53*, 9938–9941.

(2) Pedregosa, F.; Varoquaux, G.; Gramfort, A.; Michel, V.; Thirion, B.; Grisel, O.; Blondel, M.; Prettenhofer, P.; Weiss, R.; Dubourg, V.; Vanderplas, J.; Passos, A.; Cournapeau, D.; Brucher, M.; Perrot, M.; Duchesnay, É. Scikit-Learn: Machine Learning in Python. *J. Mach. Learn. Res.* **2011**, *12*, 2825–2830.

(3) Gotoh, H.; Ando, H.; Takagahara, T. Radiative Recombination Lifetime of Excitons in Thin Quantum Boxes. *J. Appl. Phys.* **1997**, *81*, 1785–1789.

(4) Rajadell, F.; Climente, J. I.; Planelles, J. Excitons in Core-Only, Core-Shell and Core-Crown CdSe Nanoplatelets: Interplay between in-Plane Electron-Hole Correlation, Spatial Confinement, and Dielectric Confinement. *Phys. Rev. B* **2017**, *96*, 035307.

(5) Kumagai, M.; Takagahara, T. Excitonic and Nonlinear-Optical Properties of Dielectric Quantum-Well Structures. *Phys. Rev. B* **1989**, *40*, 12359–12381.

(6) Beyler, A. P.; Marshall, L. F.; Cui, J.; Brokmann, X.; Bawendi, M. G. Direct Observation of Rapid Discrete Spectral Dynamics in Single Colloidal CdSe-CdS Core-Shell Quantum Dots. *Phys. Rev. Lett.* **2013**, *111*, 177401.

S6. Supplementary Tables

Parameter	Value
m_{e}	9.109×10^{-31} kg
$m_{\parallel}^{\mathrm{e}}/m_{\mathrm{e}}$	0.27
$m_{\mathrm{z}}^{\mathrm{e}}/m_{\mathrm{e}}$	0.4
L_x, L_y	20 nm
L_z	1.2154 nm
d_{shell}	3.5 nm
$\varepsilon_{\mathrm{CdSe}} = \varepsilon_{\mathrm{CdS}} = \varepsilon_1$	10
ε_2	2

Table S1. Parameter values used for the single-electron wave-function calculations described in Section S4.

S7. Supplementary Figures

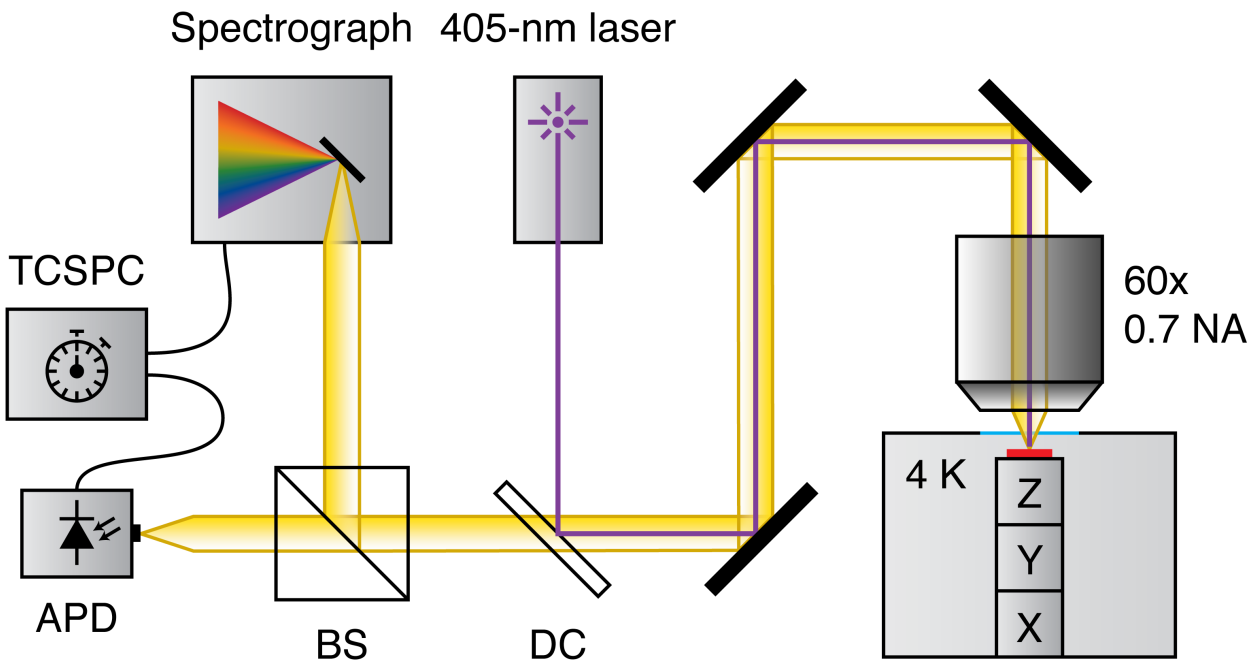

Figure S1. The experimental setup used to characterize the photoluminescence properties of individual CdSe/CdS core/shell nanoplatelets. The sample is mounted on a stack of piezo actuators (labelled X, Y, and Z) inside a cryostat. To excite the NPLs, we direct a single-mode 405-nm laser with a dichroic beam splitter through a 60× long working distance objective (0.7 NA). NPL emission is collected with the same objective and directed to the detectors. A 50:50 beam splitter cube sends half of the emission to the spectrograph and half of the emission to an avalanche photodiode (APD). A time-tagger box (TCSPC) is used to measure photon arrival times and ensure synchronization between the EMCCD camera behind the spectrograph and the APDs.

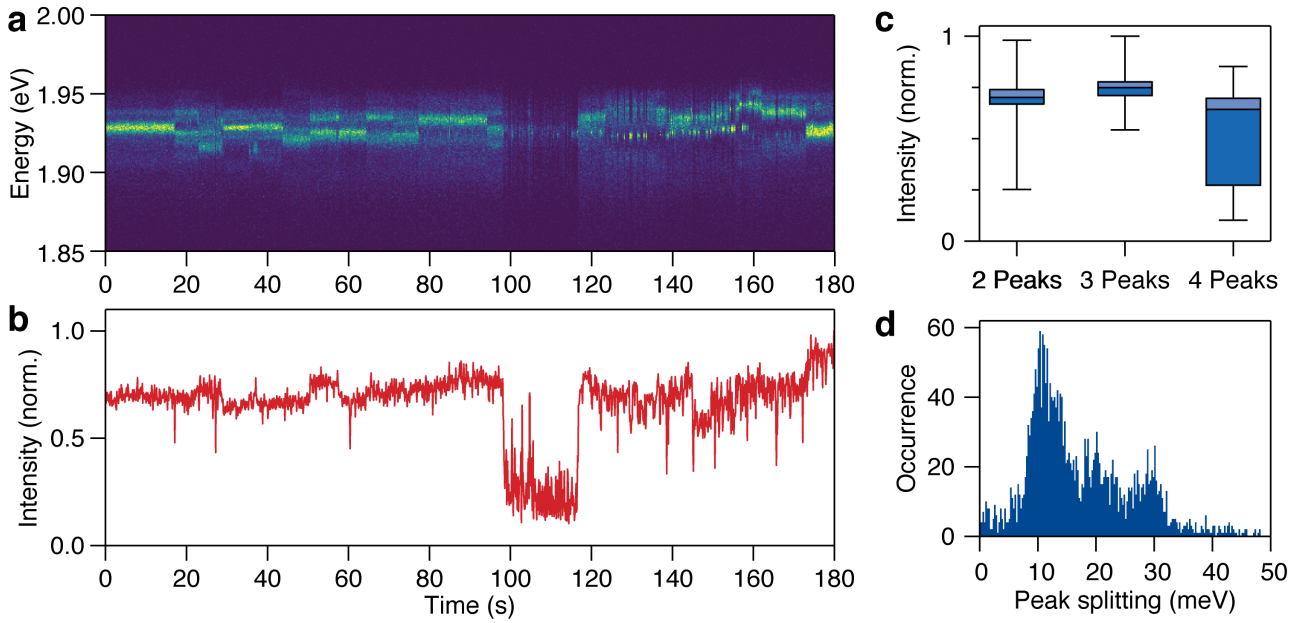

Figure S2. Additional optical data for a different individual NPL than the one characterized in detail in the main text. The data are plotted as in Figure 2 in the main text. (a) Spectral time trace. (b) Intensity trace. (c) Boxplot correlating the total emission intensity with the number of emission peaks per cluster. The horizontal line inside the box indicates the median value, the box extends from the lower to upper quartile values of the data, and the whiskers highlight the span of the datapoints. (d) Histogram of peak energy differences.

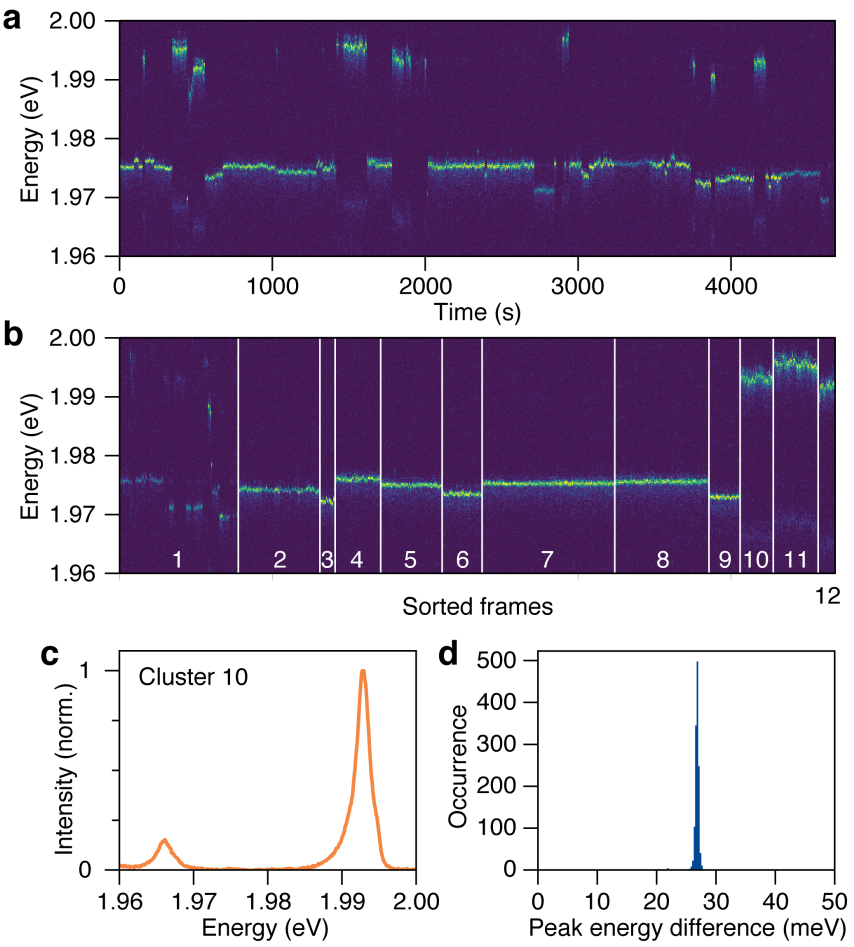

Figure S3. Spectral sorting on a time-dependent emission spectrum of an individual core/shell quantum dot (QD). (a) The emission spectrum as a function of time from the individual CdSe/CdS QD investigated in the work of Beyler et al.[6] (b) Using machine learning, the spectral time series in panel a can be sorted into a given number of emission clusters (numbered 1 through 12). (c) Average emission spectrum of cluster 10 containing a ZPL at 1.993 eV and a LO-phonon replica at 1.966 eV. The energy difference between the two peaks matches the 27 meV that corresponds to the LO-phonon energy in CdSe. (d) Histogram of all peak energy differences observed in the dataset from panel a that matches the peak energy difference that would be expected from coupling to LO phonons. The frames from cluster 1 were excluded when constructing the histogram because it was not possible to obtain a correct estimate of the number of emission peaks for this cluster.

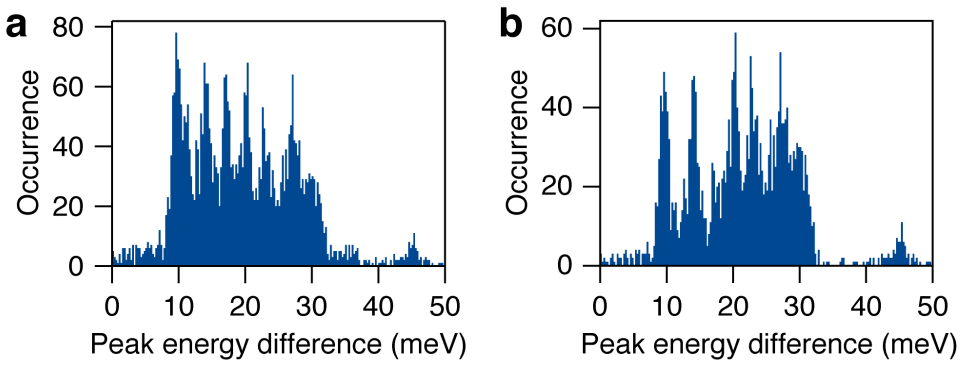

Figure S4. Histograms of all peak energy differences observed in the dataset from Figure 1b. (a) Histogram considering all peak energy differences that are observed (same data as in Figure 2g of the main text). (b) Histogram constructed by only taking the peak energy difference from the highest-energy peak.